IASMiRT

SMiRT 26
50 Anniversary Berlin/Potsdam

Transactions, SMiRT-26
Berlin/Potsdam, Germany, July 10-15, 2022
Special Session: Overview of the work done in the OECD SOCRAT benchmark dedicated to the beyond design seismic behavior assessment of crane bridges

SOCRAT Benchmark: Seismic Analyses of an Overhead Crane in LS-DYNA

Sara Ghadimi Khasraghy[1], Jan Attinger[2], Christian Schneeberger[3], Peter Rangelow[4]

[1] Project Manager, Basler & Hofmann AG, Consulting Engineers, Zurich, Switzerland, (Sara.Ghadimi@baslerhofmann.ch)
[2] Engineer, Basler & Hofmann AG, Consulting Engineers, Zurich, Switzerland
[3] Deputy Section Head, Civil Engineering Section, Swiss Federal Nuclear Safety Inspectorate ENSI, Brugg, Switzerland
[4] Senior Expert, Basler & Hofmann AG, Consulting Engineers, Zurich, Switzerland

ABSTRACT

The SOCRAT international benchmark (Seismic simulation of Overhead CRAne on shaking Table), organised by the OECD-NEA (Nuclear Energy Agency) in collaboration with IRSN (Institut de Radioprotection et de Sûreté Nucléaire) and EDF (Electricité de France), was launched in 2020. The benchmark aims at identifying the best modelling practices of bridge cranes. The project includes a selected set of tests from an experimental campaign on a scaled model of an overhead bridge crane, carried out in 2015, on the shaking table of the French Alternative Energies and Atomic Energy Commission (CEA).

In the first phase (Stage 1), analysis results of comprehensive finite element models of the overhead crane are calibrated by simulating selected experimental tests of the SOCRAT benchmark. Blind calculations for high seismic intensities are performed in the second phase (Stage 2), in which the relevant parameter are chosen based on the calibrations of Stage 1. The challenges in modelling the seismic structural response of the bridge crane, including the contact dissipative phenomena such as sliding friction and uplift, are discussed on the basis of a comparison between calculated and measured data. This paper outlines the contribution of the Swiss Federal Nuclear Safety Inspectorate (ENSI) and its consultant Basler & Hofmann AG to the SOCRAT benchmark.

INTRODUCTION

Overhead cranes are lifting and transfer equipment usually installed in industrial buildings, including the nuclear industry. In case of the safety assessment of nuclear power plants (NPPs), the seismic response of the cranes is of concern because they are relevant risk contributors in case of an earthquake. It is of importance to have accurate and reliable simulation practices to predict the nonlinear dynamic behaviour and eventually their failure probability of the overhead cranes.

The SOCRAT international benchmark, launched in 2020, aims at identifying the best modelling practices of the bridge cranes, as well as at identifying their relevant failure criteria. Twenty-two teams from eight nations have participated in this project. The teams come from various backgrounds, including engineering/consulting companies, software companies, research facilities/academy, regulators, and industry/operators. The Swiss Federal Nuclear Safety Inspectorate (ENSI) participated in this benchmark with three teams of experts from Stangenberg and Partner Ingenieur-GmbH (Germany), Basler & Hofmann AG (Switzerland), and Principia Ingenieros Consultores SA (Spain). The present article outlines the

contribution of the Swiss Federal Nuclear Safety Inspectorate (ENSI) and its consultant Basler & Hofmann AG to the calibration calculation as well as to the blind predictions of the SOCRAT benchmark.

The SORCAT benchmark project includes a selected set of tests from an experimental campaign on a scaled model of an overhead bridge crane, carried out in 2015, on the shaking table of the French Alternative Energies and Atomic Energy Commission (CEA).

Modelling of seismic structural response of the overhead cranes under seismic excitation is challenging due to the strong nonlinear behaviour at the wheel-to-rail interface. In particular, for the locked-wheel-to-rail interfaces sliding, lateral impact as well as the uplift of the trolley or crane bridge require careful consideration. According to the benchmark organizers, the anchoring of the cranes constitutes a primary cause of failure. Another cause of failure can be excessive trolley uplift or lateral deformation of the girder beams that may eventually lead to derailing of the trolley or the bridge crane.

EXPERIMENTAL EXERCISES AND NUMERICAL SIMULATION TASKS

The overhead crane mock-up is a 1/5 scaled model of a 22.5 m long crane bridge. The different structural components of the mock-up are: trolley, rails, wheels, girder beams, end truck beams, runway beams, and load cells mounted at the supports between the shaking table upper plate and the crane bridge mock-up (Figure 1).

Figure 1. Overhead crane mock-up on the shaking table

The benchmark comprises of two stages, see Table 1. In the seven exercises of the first stage (Stage 1, Exercises 1 – 7) participants calibrated their modelling assumptions using modal and transient analyses (for both low and high seismic intensities) by comparing the numerical results with the measurements. In the five exercises of the second stage (Stage 2, Exercises 8 – 12), the predictive capabilities of the numerical models are assessed using blind nonlinear simulations at high seismic intensities. The exercises differ in the position of the trolley and the crane bridge (centred or decentred) and the setting of the wheels (whether they can roll or not) of the trolley and the bridge crane (mixed or sliding wheel configurations), see Figure 2. The sliding wheels configuration corresponds to a setup where all eight wheels are fixed (i.e. cannot roll) and can only slide (with friction) on their rails. In the mixed wheels configuration four wheels can slide and the other four can roll (see Figure 2, right).

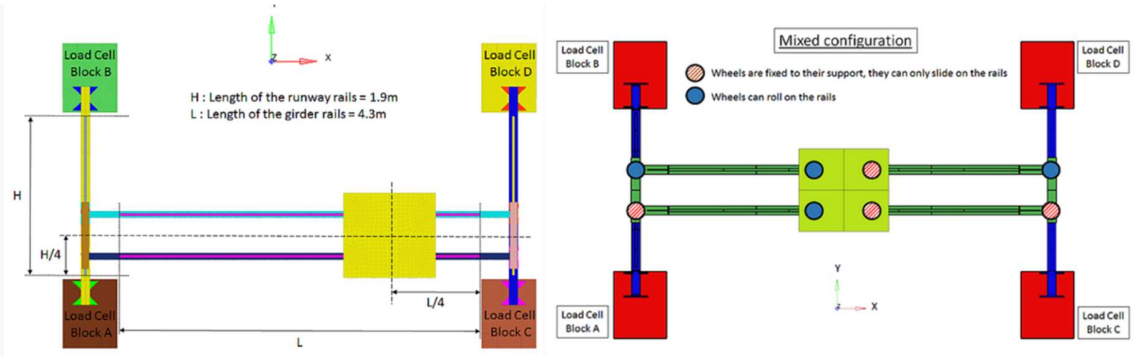

Figure 2. Decentred mock-up (left) und mixed wheels configuration (right)

Table 1: Overview of SOCRAT benchmark stages and exercises

Stage 1		Stage2	
Ex. 1 - 3	Model calibrations of the load cells, runway beam & the mock-up	Ex. 8	2D Input (PGA = 1.5 g), centred, mixed wheels
Ex. 4	Merged with Exercise 5	Ex. 9	2D Input (PGA = 1.5 g), centred, sliding wheels
Ex. 5	Friction & damping calibration, pulse, centred, sliding & mixed wheels	Ex. 10	2D Input (PGA = 1.5 g), decentred, sliding wheels
Ex. 6	Local shock calibration, 3D Input (PGA = 1.0 g), decentred, sliding wheels	Ex. 11	2D Input (PGA = 1.5 g), decentred, mixed wheels
Ex. 7	High level calibration, 3D Input (PGA = 0.5 g), centred, sliding wheels	Ex. 12	3D Input (PGA = 1.0 g), centred, mixed wheels

Note: PGA = Peak Ground Acceleration

NUMERICAL MODELS

The following subsections describe basic analysis assumptions that pertain to all simulations. Material assumptions, loading and support conditions are described in detail.

Methodology and Analysis Assumptions

Numerical simulations are carried out on three-dimensional (3D) finite element models using implicit and explicit capabilities of the LS-DYNA software (R11.0 and R 12.0).

The shaking table is assumed to provide sufficient stiffness to be considered rigid, so that the interaction between the shaking table and the mock-up can be neglected. This interaction is not expected to affect the results, because of the relatively small self-weight of the mock-up compared to the maximum loading capacity of the shaking table. Additionally, the fixture (i.e. connecting bolts) of the load cells to the shaking table is assumed to provide sufficient lateral stiffness so that the lateral displacements and vibrations of the mock-up are not significantly influenced.

Element Types and Material Models

Two final models with different levels of detail were developed for the whole mock-up bridge crane, which included a combination of beam, shell, solid, and spring elements. The so-called "simplified model" uses mostly beam elements with a combination of uniaxial gaps and sliders for the wheel-rail contact and serves for comparison and verification purposes. A final detailed model, referred here as “blind prediction model” is developed and applied for the blind predictions of Stage 2 based on the calibration calculations of Stage 1 (Figure 3). The trolley, the rails, as well as the wheels are represented by solid elements in this model. The girder beams, end truck beams and the runway beams are modelled with shell elements.

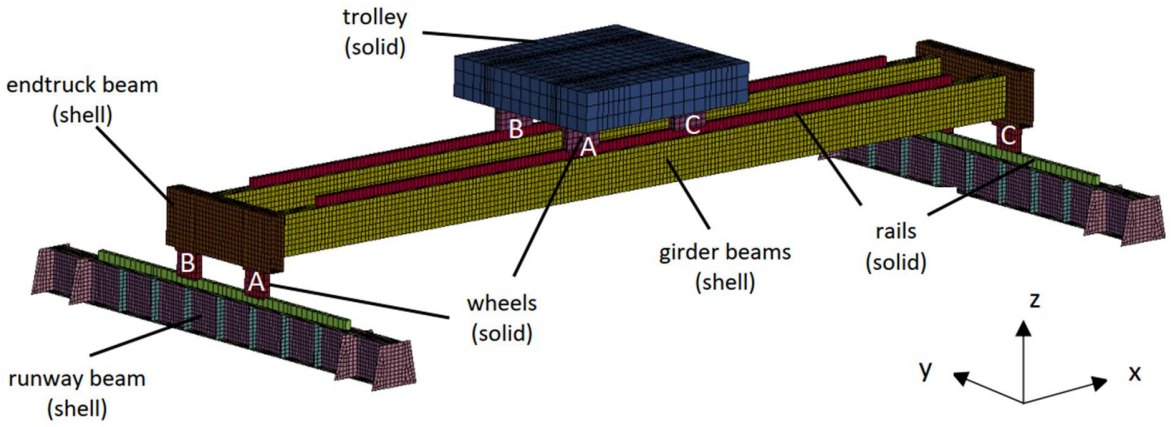

Figure 3. Finite element "blind prediction model" of the bridge crane in LS-DYNA

Materials, Loading and Support Conditions

Linear elastic material behaviour is assumed for all the steel parts of the equipment. In the detailed “ blind prediction model” the movements of the lower nodes of the runway beams, where they connect to the upper plate of the load-cell block, are blocked.

The loading is applied as acceleration time histories to the selected nodal sets. Contact surfaces incorporating friction coefficients are defined at the interface of the trolley wheels and girder beam rails, as well as between the end truck beam wheels and the runway beam rails.

PREDICTED ANALYTICAL RESULTS AND COMPARISON WITH EXPERIMENTAL DATA

To confirm the applicability of the applied numerical analysis method, comparison of selected calculated results to the experimental data of each stage is shown hereafter.

Stage 1: Calibration Calculations

The first three exercises deal primarily with the modal calibrations of the crane bridge and its components. The eigenfrequencies of the whole bridge crane using the detailed model are shown in Figure 4. The comparison of the first natural frequency of the load cell block in Exercise 1 (389 Hz for the load cell block fixed at the bottom) to the frequencies of the entire crane in Exercise 3 confirms that the load cell blocks are very stiff and have a negligible influence on the fundamental frequencies of the entire system. Therefore, the load cell blocks are assumed to be rigid and the blind prediction model does not incorporate them. The computed eigenfrequencies under this assumption match reasonably well with the experimental values (deviations smaller than 10%).

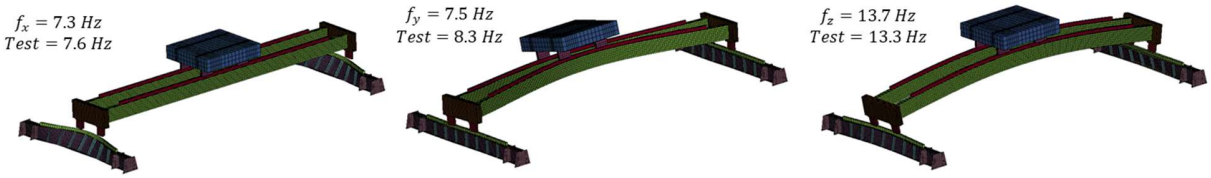

Figure 4. Modal analysis of the overhead crane (Exercise 3), first three eigenmodes of the detailed model without load cell blocks (assumed as rigid)

Exercise 5 (merged with exercise 4) explores the friction behavior at the wheel-to-rail interface. Unidirectional pulses in horizontal directions were used to trigger sliding motion. As a first approach, the contact behavior was modeled with unidirectional gap and slider elements (simplified model). However, the sliding motion measured on the mock-up could not be reproduced with the simplification of unidirectional sliding parallel to the rails. A detailed model (blind prediction model in Figure 3) was thus developed that uses a penalty-based contact algorithm for the wheel-to-rail interface, that allows sliding to take place both along and lateral to the rail, where the lateral sliding is restricted by the gap relative to the wheel flanges.

The relative displacement time history of the trolley wheels obtained from this detailed model matches the measurements as shown in Figure 5. Assuming a lower friction coefficient for the endtruck wheels than for the trolley wheels causes the endtruck wheels to slide first (lateral sliding), which corresponds to a translation of the whole crane bridge. The along the rail sliding movement of the trolley with respect to its substructure only starts after t = 7.6 s when the gap (lateral clearance between wheel flange and rail) of the endtruck wheels is closed.

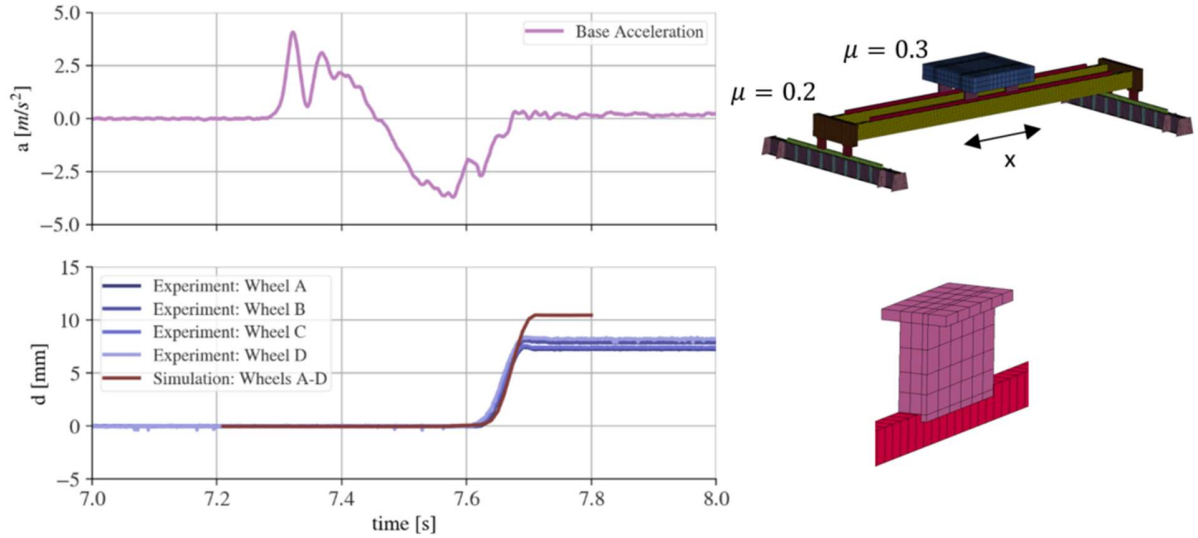

Figure 5. Relative displacement (sliding motion) in x-direction at the trolley wheels for Exercise 5

In Exercise 6, a 3D seismic signal with PGA = 1 g was imposed by the shaking table. The sliding wheels configuration was set up, in combination with eccentric positions of the trolley and the bridge crane according to Figure 2. Exercise 6 was intended for studying the local shock parameters of the collision between the wheels and the rails. However, this exercise was primarily useful for a general model check since no uplift was observed. The results of this exercise are not discussed here.

Exercise 7 aimed at high-level calibration by applying a 3D seismic signal with PGA of 0.5 g and considering the centered wheel sliding configuration. In order to save computation time only 5 seconds of the input signal were considered in the analyses. This input time history covers the significant duration where most of the energy is accumulated (i.e. the strong motion phase). Assuming the same coefficients of friction as in Exercise 6, the relative displacement time histories of the endtruck wheels agreed reasonably well with the measurements as shown in Figure 6 (lower plot). However, the measurements show low residual displacements for wheels A and B.

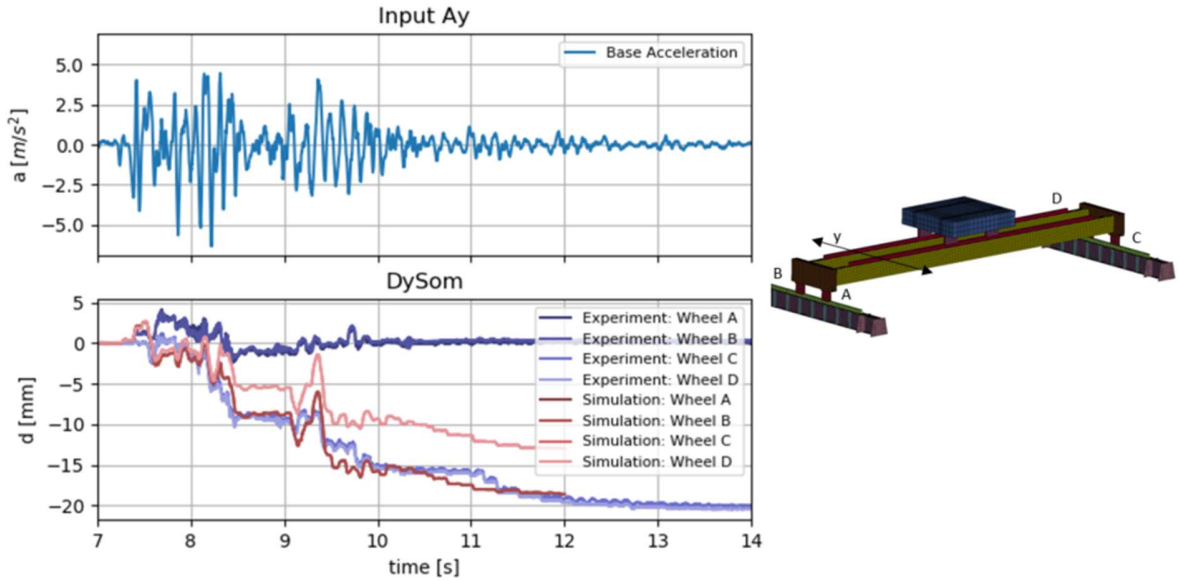

Figure 6. Input base acceleration and relative displacement time histories of endtruck wheels (along the rail) for Exercise 7

In addition to the analysis of the along the rail displacement time histories of the endtruck wheels, vertical acceleration time histories of the trolley are compared in Figure 7. The uplift phenomenon can be identified in the time history data, as the signal is bounded downwards by - 9.81 m/s^2. When analyzing the signal in the frequency domain using a power spectrum, the fundamental frequency in the vertical direction can be observed between 13 and 14 Hz. In general, the simulation captures the frequency characteristics of the response with high accuracy in the displayed frequency range from 0 to 100 Hz.

A major goal of the Stage 1 was the calibration of the modeling assumptions of the wheel-rail contact. However, it was hardly possible to find a single combination of friction coefficients for the wheels providing a good match between simulation and experiments for all three exercises 5, 6, and 7. It should be noted that some damage to the rails was observed during the experiments, in addition to the local wheel damage. These damages, which may cause a variation of the friction coefficients between the exercises, were not systematically documented. Hence, the benchmark participants could not calibrate the friction coefficients between the exercises based on the associated suffered rail and wheel damage. This may lead to different friction coefficients on opposite sides of the trolley or runway beam wheels (or even at each of the eight wheels).

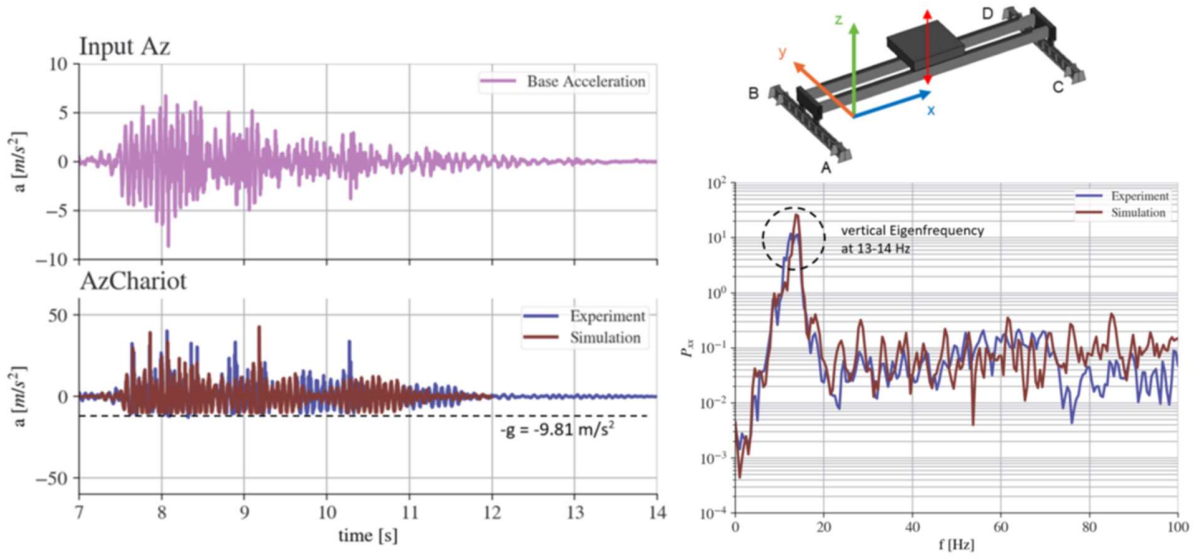

Figure 7. Vertical acceleration at the trolley for the 3D seismic excitation of Exercise 7

Stage 2: Blind Predictions

After calibration of the numerical models in Stage 1, five blind prediction exercises were carried out in Stage 2 (Exercises 8 to 12, see Table 1). They aimed at evaluating the nonlinear response of the bridge crane mock-up under high intensity seismic loading and included "centred" and "decentred" positions of the trolley and the bridge crane under both "sliding" and "mixed" wheels configurations. The measured data of these exercises was not provided in advance. Only seismic signals at the shake table were given as input data for the simulation.

The blind computations in Stage 2 are performed with the blind prediction model calibrated in Stage 1 (Exercises 5, 6 and 7). A friction coefficient of $\mu = 0.3$ was assumed for the wheels of the trolley on the girder rail, whereas $\mu = 0.2$ was assumed for the wheels of the endtruck on the runway rail.

The results of the blind nonlinear simulations are compared to the experimental measurements in order to explore the influence of the modelling assumptions on the predictive ability of the numerical models. Comparisons of selected results are discussed here.

The acceleration signals of Exercises 8, 10 and 11 were found to be almost identical. The signals of Exercises 9 and 12 were also identical in shape, but with different amplitude scales (a scale factor of -1 for Exercise 9 and a factor of -2/3 for Exercise 12 with respect to the signal of the Exercise 8).

For the blind prediction model, a friction coefficient of $\mu = 0.3$ was chosen for the trolley wheels on the girder rail, whereas $\mu = 0.2$ was assumed for the bridge crane wheels on the runway rail. The simulations were performed for the strong motion phase, with the time frame from 6 to 11 s similar to the calibration calculations, where more than 95% of the Arias Intensity of the signal is contained.

Selected results of the Exercise 9 are compared with the experimental data and discussed. The relative displacements of the trolley (x-direction) and the bridge crane (y-direction) are compared with the measurements in Figure 8.

The simulation is able to predict relevant sliding motion characteristics, such as the magnitude and direction of the sudden sliding movements in both directions. For example, the simulation predicts a sudden sliding of the trolley of 24 mm in negative x-direction at t = 7.3 s, which agrees well with the measurement (see Figure 8, left). For the motion of the bridge crane in y-direction, both the simulation and the measurement show diverging displacements for the sides A-B and C-D over time, i.e. the bridge crane is rotating about the vertical axis (yawing) during this excitation. Whereas the measurements show a residual displacement of over 60 mm between the two sides, the simulation predicts a residual displacement of only 20 mm (see Figure 8, right).

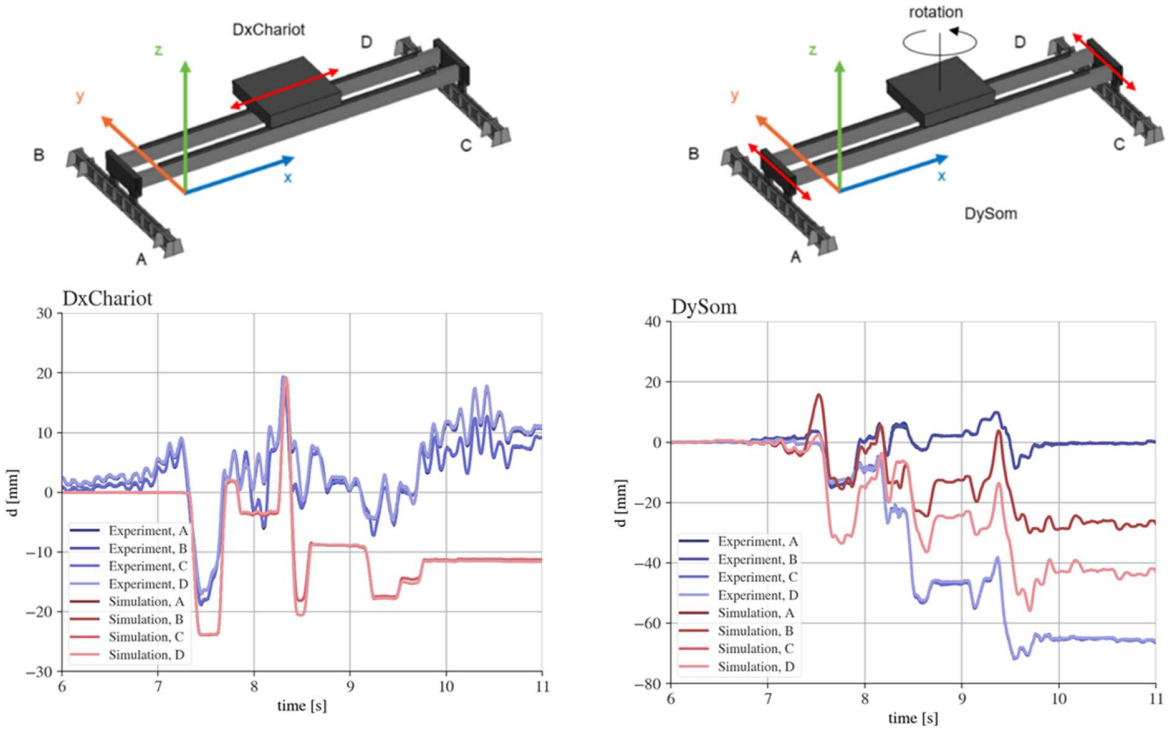

Figure 8. Blind prediction of the relative displacement (sliding motion) of the trolley (left plot) and bridge crane (right plot) for 2D seismic excitation (Exercise 9)

The vertical displacements of the girder beam at mid-span are compared in Figure 9. The comparison of displacement time histories shows good agreement on frequency and phase. However, the amplitudes of the simulation tend to be smaller. Comparing the power spectral densities of the simulated and measured time histories, the signals align well around the fundamental eigenfrequency in vertical direction, which is between 13-14 Hz.

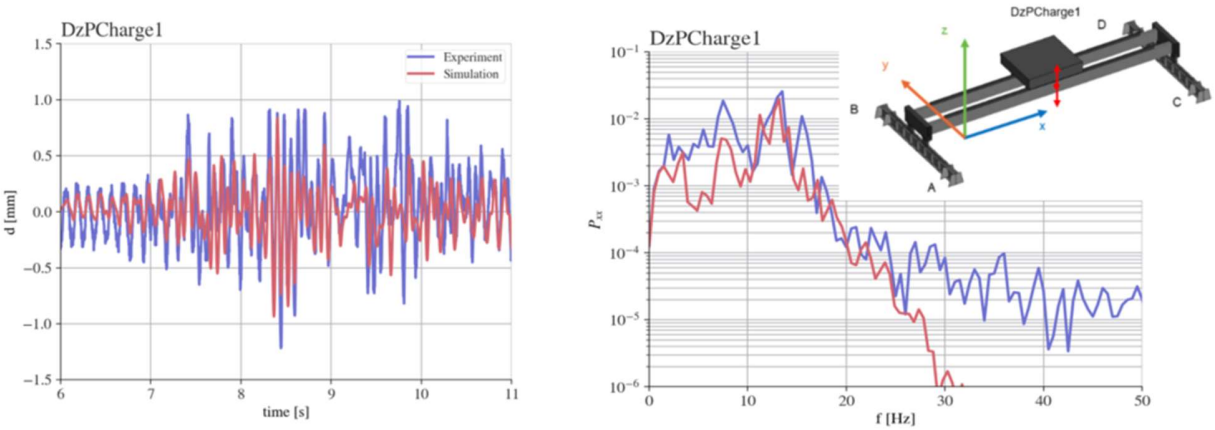

Figure 9. Vertical displacement of the girder beam mid-span for 2D seismic excitation (Exercise 9)

The measured reaction forces in the support position "A" are compared in Figure 10 with the calculated forces of the blind prediction model, as well as with the forces obtained from the simplified model with linearized contacts (hinge connections at the wheel-rail interface).

The simplified linear model predicts reaction forces in x, y and z-direction that are between 40 and 60 kN. For the blind prediction model, the forces are between 10 and 20 kN and thus at least by a factor of two smaller than the forces obtained from the simplified linear model. The maximum measured horizontal forces at support A are Fx = 23.6 kN and Fy = 17.1 kN, and hence deviate about 15% from the blind prediction results. In vertical direction, the deviation is larger and could be caused by an overestimation of the assumed damping (ζ = 2 %) in the simulation.

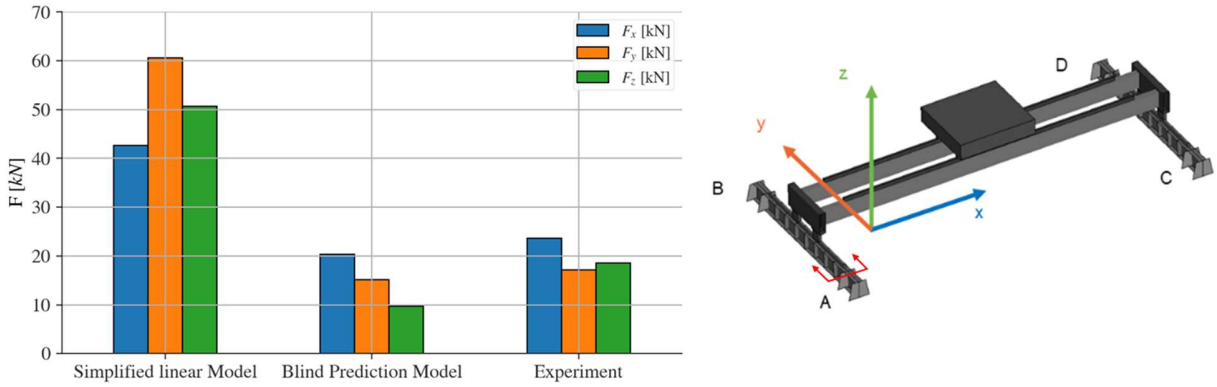

Figure 10. Reaction forces at support A for 2d seismic excitation (Exercise 9)

CONCLUSION

In the first phase (Stage 1) of the SOCRAT benchmark, the analysis results of a comprehensive finite element model of the overhead crane are calibrated by modal analyses as well as by simulation of selected experimental tests. Calibration of the modelling assumptions of the wheel-rail contact was the main goal of the Stage 1 simulations. However, it was hardly possible to find a single combination of friction coefficients for the wheels providing a good match between simulation and measured data for all Stage 1 exercises.

Blind prediction calculations for high seismic intensities are performed in the five exercises of the second phase (Stage 2), in which the relevant model parameter are chosen based on the calibrations of the Stage 1.

The challenges in modeling the seismic structural response of the crane bridge, including the contact dissipative phenomena such as the sliding friction and uplift, are discussed on the basis of a comparison between calculated and measured data.

The fundamental frequencies of the mock-up are accurately estimated by a modal analysis with deviations smaller than 10 % from the measured frequencies. For 2D and 3D seismic excitations, a more pronounced rotation about the vertical axis (yawing) of the bridge crane was observed in the experiments than the simulation predicted. This observation suggests that an assumed uniform friction coefficient for the wheels might be way too simple idealization for some of the simulated exercises. However, allowing for a more sophisticated friction model, e.g. individual friction coefficients for each wheel, bears the risk of "over-calibration". On the other hand, some damage to the rails and wheels was observed during the experiments. These damages, which may cause a variation of the friction coefficient between the exercises, were not systematically documented. Hence, the benchmark participants could not calibrate the friction coefficients between the exercises based on the associated suffered rail and wheel damage. Moreover, the test campaign showed that the test runs with same initial and boundary conditions produced diverging results. Therefore, an exact match between simulation and experiment could not be expected.

For the provided excitation signals, the uplift of the trolley wheels from the rails could be observed in both the measured and simulated acceleration time histories. However, the calculated vertical gap did not exceed 3 mm (Exercise 12) and does not pose a risk of derailing of the trolley at this excitation level, since the height of the wheel flange is 10 mm.

The maximum horizontal forces in the supports could be accurately predicted with deviations around 15 % for the Exercise 9. A slight underestimation of the reaction forces was expected, as in the simulation the section forces were evaluated at the end of the runway beams and do not incorporate the inertia of the load cells. For the vertical reaction forces a larger deviation was registered, presumably because of overestimation of the assumed damping (ζ = 2 %) in the simulation. For the blind prediction model, the reaction forces are at least by a factor of two smaller than the forces obtained from the simplified linear model, which demonstrates the importance of considering contact nonlinearities.

REFERENCES

Livermore Software Technology Corporation (LSTC), an Ansys Company (2020). LS-DYNA Software, Version LS-DYNA R11/R12, Keyword and Theory Manuals.

SOCRAT Benchmark, First announcement, 11.06.2020, and the project website: www.socrat-benchmark.org